Water Stress Detection Under High Frequency Sprinkler Irrigation with Water Deficit Index

Paul D. Colaizzi[1]; Edward M. Barnes[2]; Thomas R. Clarke[3]; Christopher Y. Choi[4]; Peter M. Waller[5]; J. Haberland[6]; and Michael Kostrzewski[7]

Abstract: A remote sensing package called the agricultural irrigation imaging system (AgIIS) aboard a linear move irrigation system was developed to simultaneously monitor water status, nitrogen status, and canopy density at one-meter spatial resolution. The present study investigated the relationship between water status detected by AgIIS and soil moisture for the 1999 cotton (*Gossypium hirsutum*, Delta Pine 90b) season in Maricopa, Ariz. Water status was quantified by the water deficit index (WDI), an expansion of the crop water stress index where the influence of soil temperature is accounted for through a linear mixing model of soil and vegetation temperature. The WDI was best correlated to soil moisture through the FAO 56 water stress coefficient K_s model; stability correction of aerodynamic resistance did not improve correlation. The AgIIS did provide field images of the WDI that might aid irrigation scheduling and increase water use efficiency.

Introduction

Remote sensing is an efficient method for detecting crop water stress on a site-specific basis if canopy temperature measurements are available at sufficient spatial resolution (Jackson 1984; Moran et al. 1997). Satellite and aircraft remote sensing platforms generally lack the timeliness, repeat frequency, or spatial resolution required for irrigation management, and data acquired by these platforms carry a greater processing requirement than if acquired from the ground (Moran 1994). Self-propelled center pivot and linear move irrigation systems can provide a platform for ground-based remote sensing (Phene et al. 1985) and variable-rate application needed for site-specific irrigation management (Sadler

[1]Agricultural Engineer, Conservation and Production Research Laboratory, U.S. Dept. of Agriculture/Agricultural Research Service, P.O. Drawer 10, Bushland, TX 79012.

[2]Agricultural Engineer, U.S. Water Conservation Lab., U.S. Dept. of Agriculture/Agricultural Research Service, 4331 East Broadway, Phoenix, AZ 85040.

[3]Physical Scientist, U.S. Water Conservation Lab., U.S. Dept. of Agriculture/Agricultural Research Service, 4331 East Broadway, Phoenix, AZ 85040.

[4]Associate Professor, Dept. of Agricultural and Biosystems Engineering, Univ. of Arizona, Tucson, AZ 85721.

[5]Associate Professor, Dept. of Agricultural and Biosystems Engineering, Univ. of Arizona, Tucson, AZ 85721.

[6]Research Associate, Dept. of Agricultural and Biosystems Engineering, Univ. of Arizona, Tucson, AZ 85721.

[7]Research Associate and Graduate Student, Dept. of Agricultural and Biosystems Engineering, Univ. of Arizona, Tucson, AZ 85721.

et al. 2000). Since these systems pass over a field at regular intervals, an on-board remote sensing system conceivably could provide information on crop conditions that meets repeat frequency and spatial resolution requirements. The availability of global positioning systems (GPSs) and high-speed personal computers in recent years would allow on-site processing of data at high spatial resolution within minutes, fulfilling the timeliness requirement.

We developed a remote sensing package called the agricultural irrigation imaging system (AgIIS) designed to simultaneously monitor water status, nitrogen status, and crop growth at 1 m spatial resolution. The AgIIS contains a nadir-looking group of sensors that are transported by a cart that moves along a track; the track is mounted to a two-span linear move irrigation system (see Colaizzi 2001 for illustration). The sensors detect reflectance in four bands, and an infrared thermometer (IRT) measures the surface temperature, described further in the Experimental Methods section.

Water status using an IRT is commonly quantified using the crop water stress index (CWSI) (Idso et al. 1981; Jackson et al. 1981). Appreciable errors in the CWSI are possible when the soil beneath a crop appears in the IRT field of view because soil temperature is generally different from canopy temperature. The CWSI, therefore, is not valid unless canopy cover is full when a nadir-looking IRT is used. The CWSI may be valid for partial canopy cover if off-nadir IRT measurements are possible; however, Kimes et al. (1980) reported that radiant temperatures of non-Lambertian canopies were highly dependent on view angle. In either case, soil background may still appear during times of water stress because of leaf wilt (Jackson et al. 1986).

Moran et al. (1994) addressed the influence of soil background by accounting for soil temperature using the same energy balance principles used in the CWSI, and defined the water deficit index (WDI). Clarke (1997) demonstrated that the WDI could detect differences in water status using data from airborne multispectral and thermal sensors that were flown over a muskmelon farm west of Phoenix, Ariz. In the present study, the WDI was used instead

of the CWSI since the AgIIS sensors view the field surface at nadir. The objectives of this study are to test the ability of AgIIS to detect differences in water status, and to investigate the relationship between the WDI and soil moisture. The development and calculation of the WDI are described next.

Water Deficit Index

The WDI quantifies the relative rate of latent heat flux leaving a surface by evaporation and transpiration, where the surface is a mixture of vegetation and bare soil. The WDI is defined as 0.0 for well-watered conditions (i.e., a completely wet surface where latent heat flux is limited only by atmospheric demand) and 1.0 for no available water (i.e., a completely dry surface where there is no latent heat lost to the atmosphere). This definition is analogous to the CWSI where the surface is restricted to full vegetation (canopy) cover. Latent heat flux is related to the temperature of the surface by the energy balance, and surface temperature can be measured with an IRT.

For a given set of aerodynamic and radiation conditions, the surface temperature will have a theoretical upper and lower limit, depending on water available for transpiration and evaporation. A measurement of surface temperature using an IRT should fall somewhere between these upper and lower limits. During afternoon hours when atmospheric demand is at a diurnal maximum, the upper and lower surface temperature limits are generally greater and less than air temperature, respectively. Taking the surface–air temperature difference $(T_s - T_a)$, the respective upper and lower limits are generally positive and negative. The WDI is defined as

$$\text{WDI} = \frac{(T_s - T_a)_m - (T_s - T_a)_{ll}}{(T_s - T_a)_{ul} - (T_s - T_a)_{ll}} \tag{1}$$

where m designates $(T_s - T_a)$ measured by an IRT, ul and ll = theoretical upper (dry) and lower (wet) limits of $(T_s - T_a)$; respectively, and all temperatures are in units of °C.

The surface temperature T_s terms in Eq. (1) are composites of both bare soil and vegetation surface temperatures that appear in an IRT field-of-view. Moran et al. (1994) presented assumptions with supporting data that the bare soil and vegetation components can be partitioned as a linear function of the fraction of vegetation cover for irrigated crops. The upper and lower $(T_s - T_a)$ limits in Eq. (1) become

$$(T_s - T_a)_{ll} = f_c (T_s - T_a)_{wv} + (1 - f_c)(T_s - T_a)_{ws} \tag{2}$$

$$(T_s - T_a)_{ul} = f_c (T_s - T_a)_{dv} + (1 - f_c)(T_s - T_a)_{ds} \tag{3}$$

where f_c = fraction of vegetation cover appearing within in the IRT field-of-view, wv = wet vegetation (well-watered canopy); ws = wet bare soil; dv = dry vegetation (completely water stressed canopy); and ds = dry bare soil. The f_c term can be monitored by reflectance in the red and near-infrared bands through a spectral vegetation index, such as the normalized difference vegetation index (NDVI); (Rouse et al. 1974) or the soil adjusted vegetation index (Huete 1988). The $(T_s - T_a)_n$ terms in Eqs. (2) and (3) are calculated based energy balance equations (see Appendix).

Although the WDI is analogous to the CWSI, the WDI as defined is not strictly related to crop water stress because it also accounts for evaporation from bare soil. Consequently, a WDI value greater than zero does not necessarily indicate that crop transpiration rates are below atmospheric potential (i.e., water stress), as would be the case for the CWSI. It may result, for example, from both nonwater stressed vegetation and a partial or completely dry soil surface appearing in the IRT field-of-view.

Water Deficit Index and Soil Moisture Relations

Moran et al. (1994) give an alternative definition of the WDI in terms of latent heat flux

$$\text{WDI} = 1 - \frac{\lambda \text{ET}_c}{\lambda \text{ET}_p} \tag{4}$$

where λET_c and λET_p = instantaneous actual and potential evapotranspiration (W m^{-2}), respectively, of a surface. Eq. (4) is identical to the CWSI, as defined by Jackson et al. (1981) and used by Colaizzi et al. (2003) in relating the CWSI to soil moisture. The CWSI, however, pertains only to full canopy cover where plant transpiration dominates the energy balance of the measured surface temperature. As mentioned before, the WDI also includes a soil evaporation component in the measured surface temperature, which becomes significant for partial canopy cover and is implied in Eq. (4). With this distinction noted, the WDI can be related to soil moisture in the same manner as the CWSI was in Colaizzi et al. (2003) by substituting $(\lambda \text{ET}_c / \lambda \text{ET}_p)$ with $(\text{ET}_c / \text{ET}_p)$ in Eq. (4), where the latter is the daily latent heat flux ratio. Since a soil evaporation component is also implied in $(\text{ET}_c / \text{ET}_p)$, the resulting expression is termed the soil water deficit index (SWDI)

$$\text{SWDI} = 1 - \frac{\text{ET}_c}{\text{ET}_p}. \tag{5}$$

The ET_c term in Eq. (5) was calculated using the dual crop coefficient procedure of the Food and Agriculture Organization Paper No. 56 (FAO 56) (Allen et al. 1998), given by

$$\text{ET}_c = \text{ET}_o (K_{cb} K_s + K_e) \tag{6}$$

where ET_o = reference evapotranspiration (mm day^{-1}), K_{cb} = basal crop coefficient; K_s = water stress coefficient; and K_e = soil evaporation coefficient. The ET_p term in Eq. (5) is the maximum possible value of ET_c. This occurs when $K_s = 1$ and $(K_{cb} + K_e)$ reach an upper limit $(K_{c\text{-max}})$ that is constrained only by atmospheric demand (Allen et al. 1998), and ET_p is

$$\text{ET}_p = \text{ET}_o K_{c\text{-max}} \tag{7}$$

Substituting Eqs. (6) and (7) into Eq. (5) and simplifying, the SWDI can be expressed in terms of FAO 56 parameters

$$\text{SWDI} = 1 - \frac{K_{cb} K_s + K_e}{K_{c\text{-max}}} \tag{8}$$

Comparison of Eqs. (8)–(18) in Colaizzi et al. (2003) shows that the SWDI is different from its CWSI-based companion expression, the soil water stress index (SWSI) because the SWDI includes soil evaporation. The SWSI, however, includes a stress recovery coefficient K_{rec}. Although K_{rec} was unnecessary in the present study, which used high frequency irrigation, it could be included in the numerator of Eq. (8) for future studies if the WDI was used in conjunction with low frequency (surface) irrigation (i.e., $K_{cb} K_s K_{rec} + K_e$).

This study compared two K_s models. In the FAO 56 model, K_s is a function of the fraction of soil moisture depletion (fDEP), the sensitivity of the crop to water stress, and ET_c. Jensen et al. (1970) give a K_s model as a function of fDEP only. Both K_s models are given in Colaizzi et al. (2003), as are methods of estimating K_{cb}, which are based on cumulative growing degree days (GDDs). The K_e term was calculated based on FAO 56 procedures [Eqs. (71)–(75)]. If WDI is substituted for SWDI in Eq. (8), the WDI can be related to soil moisture through K_s.

Table 1. Crop Development Stages and Basal Crop Coefficient K_{cb}. Development Stage Nomenclature is Taken from Food and Agricultural Organization Paper 56 for Generic Crop, and Agronomic Stages for Cotton are in Parentheses

DOY	Date	Development stage	Cumulative GDD (°C)	K_{cb}
106	16 Apr	Plant		
106–152	16 Apr–1 Jun	Initial (establishment, early vegetative)	0–440	0.15
153–212	2 Jun–31 Jul	Development (vegetative, flowering, early boll formation)	440–1,320	0.15→1.17
213–241	1 Aug–29 Aug	Mid-season (late flowering, mid-late boll formation)	1,320–1,760	1.17
242–275	30 Aug–2 Oct	End (yield formation, ripening)	1,760–2,200	1.17→0.4
321	17 Nov	Harvest		

Experimental Methods

The experiment was conducted at the University of Arizona Maricopa Agricultural Center (latitude 33°04′N, longitude 111°58′W, 361 m mean sea level) in Maricopa, Ariz. Cotton (*Gossypium hirsutum*, cv. Delta Pine 90b, full season) was planted on 16 April 1999 [day of year (DOY) 106] on east–west, raised beds spaced 1.0 m apart on a laser-leveled 1.3 ha field. Plant density was estimated at 10 plants m^{-2} after establishment. The soil is classified as a Casa Grande series, with sandy loam or sandy clay loam textures (Post et al. 1988). The field was irrigated using a two-span Valley (Valmont Industries, Inc., Valmont, Neb.) linear move irrigation system with drop hoses that irrigated between the raised beds. Nitrogen was applied by injecting 32% liquid urea ammonium nitrate (UAN32) into the irrigation water.

Treatments consisted of two water levels and two nitrogen levels (2×2 factorial) replicated four times. The field was divided into a 16-plot Latin square design; each plot was approximately 20 m$\times$20 m. Treatments are designated by WN (Optimal Water, Optimal Nitrogen), Wn (Optimal Water, Low Nitrogen), wN (Acute Water Stress, Optimal Nitrogen), and wn (Acute Water Stress, Low Nitrogen). The acute water stress treatments (w) consisted of delaying irrigations twice toward the end of the development stage (vegetative, flowering, early boll development) and three times during the mid-season stage (late flowering, mid-late boll development). Irrigation amounts were increased after the delayed irrigations in an effort to bring the soil moisture levels back to those of the optimal water (W) treatments. This was to avoid chronic water stress, but institute stress events that might be characteristic of a commercial production setting when operational constraints or scheduling errors prevented a timely application. Solenoid-controlled boom sections below the main overhead pipe of the linear move varied water and nitrogen applications for individual plots. All plots were diked to prevent runoff. Water for optimal water treatment plots was metered to match evapotranspiration requirements estimated from FAO 56. Nitrogen treatments consisted of applying a total of 112 and 222 kg ha^{-1} to low and optimal plots, respectively, by 75% completion of the development stage (late vegetative). Table 1 summarizes the crop development stages during the season.

The AgIIS provided red and near infrared reflectance and surface temperature (IRT) data required for the WDI. The AgIIS sensor has four reflectance bands and one thermal (IRT) band, all nadir looking from a 4 m height above the ground with a 15° field of view, resulting in a footprint of about 1 m. Reflectance bands are green (555 nm), red (670 nm), red-edge (720 nm), and near infrared (790 nm), filtered to a 10 nm band pass about the band centers. The sensor integrated reflectance and thermal measurements over each row for about 10 ms, when triggered by an optical proximity sensor. The speed of the linear move system was adjusted so that 1 m$\times$1 m spatial resolution resulted as the sensor traversed the field. A GPS (Trimble AgGPS 132) aboard the linear move provided coordinate data so that remotely sensed data could be compiled into images of the field. Agricultural irrigation imaging system acquired field images at least weekly throughout the season, and as often as three times per week during rapid crop growth. Acquisition times began at 1,230 h (approximate solar noon) and took about 2.5 h to cover the entire field. An on-farm Arizona Meteorological Network (AZMET 1999) station provided meteorological data on an hourly basis. Rainfall was recorded by an in-field rain gage. The fraction of vegetation cover f_c required in Eqs. (2) and (3) was correlated to the NDVI (Rouse et al. 1974) by linear regression by weekly destructive plant sampling in three locations of each plot, which also gave estimates of plant height. The NDVI is ($\rho_{NIR} - \rho_{red})/(\rho_{NIR} + \rho_{red})$ where ρ is the reflectance in the red or near-infrared (NIR) bands. Volumetric soil moisture was measured and estimated between measurements using the same procedures described by Colaizzi et al. (2003).

The WDI was computed from Eq. (1) using AgIIS and meteorological data; this was compared to the SWDI computed from Eq. (8). Plot averages of WDI values for each day of an AgIIS acquisition were the basis of the comparisons to the SWDI, given in terms of slope, intercept, r^2, bias, and root mean squared error (RMSE) for each treatment. The WDI was computed using three aerodynamic resistance models (the Campbell model, with and without stability correction, and the Monteith model). The SWDI was computed using two K_s models (FAO 56 and Jensen), making a total of six comparisons. The aerodynamic resistance and K_s models used are given by Colaizzi et al. (2003). The days considered in the analysis spanned from DOY 167 to DOY 270 (vegetative, flowering, boll development, yield formation, and ripening).

Results and Discussion

Table 2 shows the seasonal totals for irrigation depths, precipitation, potential evapotranspiration (ET$_p$), crop evapotranspiration

Table 2. Total Seasonal Irrigation, Rain, Potential Crop Water Use (ET$_p$), Actual Crop Water Use (ET$_c$), Total Nitrogen Application, and Final Lint Yield for Each Treatment

Treatment	WN	Wn	wN	wn
Irrigation (mm)	1,070	1,070	1,000	1,000
Rain (mm)	150	150	150	150
ET$_p$ (mm)	1,150	1,150	1,150	1,150
ET$_c$ (mm)	1,000	1,020	910	900
Nitrogen (kg/ha)	222	112	222	112
Lint (kg/ha)	1,200	1,380	1,250	1,360

Table 3. Summary Statistics for Comparisons between Water Defecit Index and Soil Water Defecit Index Using Food and Agricultural Organization Paper 56 K_s Model

r_a Method	Treatment	n	Slope	Intercept	r^2	Bias	RMSE
No Stabil. Corr.	WN	124	1.00[a]	0.02[a]	0.87	0.015	0.071
No Stabil. Corr.	Wn	119	0.97[a]	0.03	0.86	0.018	0.069
No Stabil. Corr.	wN	118	0.97[a]	0.01[a]	0.84	0.000	0.081
No Stabil. Corr.	wn	124	0.95[a]	0.03	0.85	0.012	0.083
Campbell	WN	124	1.11	−0.06	0.86	−0.030	0.089
Campbell	Wn	119	1.07[a]	−0.04	0.84	−0.024	0.085
Campbell	wN	118	1.09	−0.07	0.84	−0.035	0.096
Campbell	wn	124	1.06[a]	−0.04	0.86	−0.019	0.089
Monteith	WN	124	0.99[a]	0.07	0.86	0.069	0.095
Monteith	Wn	119	0.95[a]	0.09	0.82	0.074	0.100
Monteith	wN	118	0.96[a]	0.07	0.80	0.057	0.102
Monteith	wn	124	0.95[a]	0.09	0.84	0.072	0.105

[a]Slopes or intercepts not significantly different from 1.0 or 0.0, respectively ($\alpha = 0.05$).

(ET$_c$), nitrogen applications, and final lint yield for each treatment. ET$_c$ and ET$_p$ were computed using Eqs. (6) and (7), respectively. Reference evapotranspiration (ET$_o$) required for Eqs. (6) and (7) was calculated using the Penman–Monteith equation for a grass reference crop with daily time steps [Eq. (6) in FAO 56]. Total irrigation plus precipitation were all similar to ET$_p$, but ET$_c$ was 13, 11, 21, and 22% less than ET$_p$ for the respective treatments (WN, Wn, wN, and wn).

Final lint yield was greater for the low nitrogen (n) than for optimal nitrogen treatments (N), and several interrelated factors may have influenced this. The greater nitrogen applications may have encouraged greater amounts of vegetation growth at the expense of boll development. The short-term induced water stress during the development (vegetative-flowering) and mid-season (flowering-boll development) stages in the acute water stress (w) treatments may have also discouraged vegetative growth, resulting in greater energy being used for boll formation. The plots exhibiting greater vegetative growth may have been more attractive to the pest *Lygus*, which was observed earlier in the season and was thought to have damaged early fruiting structures (Ellsworth and Barkley 2001). Indeed, green boll counts on the optimal treatment plots (WN) fell slightly below the other plots when infestation was observed. The first induced water stress during the vegetative stage may have encouraged greater root devel-

opment, allowing greater access to soil moisture during mid-season when bolls were forming (Doorenbos and Kassam 1979). These interactions suggest differences in root development between treatments, which complicate the relationship between canopy temperature-based indices and soil moisture (Jackson et al. 1981; Jackson 1982).

Tables 3 and 4 show summary statistics for comparisons between the WDI and the SWDI. The best comparison generally resulted between the WDI without stability correction and the SWDI using the FAO 56 K_s model (Table 3). Fig. 1 shows xy scattergrams (WDI versus SWDI) for each treatment for this comparison. Each treatment had the slope closest to unity, the highest r^2 (except for the wn treatment), the least bias (w treatments only), and the least RMSE compared to the other aerodynamic resistance and K_s combinations. The slopes were not significantly different from one; however, the intercepts for both of the low nitrogen (n) treatments were significantly different from zero ($\alpha = 0.05$). Stability correction did not improve correlation between the WDI and the SWDI. Colaizzi et al. (2003) reached the same conclusion in a similar study using the CWSI, as did Kjelgaard et al. (1996) in comparing the canopy temperature energy balance to the Bowen ratio energy balance.

Fig. 2 shows the time series of SWDI (FAO 56 K_s), WDI (no stability correction), fraction of vegetation cover f_c, irrigation

Table 4. Summary Statistics for Comparisons Between Water Defecit Index and Soil Water Defecit Index using Jensen K_s Model

r_a Method	Treatment	n	Slope	Intercept	r^2	Bias	RMSE
No Stabil. Corr.	WN	124	1.12	0.00[a]	0.86	0.030	0.080
No Stabil. Corr.	Wn	119	1.09	0.02[a]	0.85	0.038	0.078
No Stabil. Corr.	wN	118	1.09	0.01[a]	0.79	0.035	0.099
No Stabil. Corr.	wn	124	1.11	0.02[a]	0.78	0.053	0.110
Campbell	WN	124	1.25	−0.08	0.84	−0.014	0.098
Campbell	Wn	119	1.20	−0.05	0.83	−0.003	0.090
Campbell	wN	118	1.22	−0.06	0.78	0.000	0.113
Campbell	wn	124	1.24	−0.05	0.77	0.022	0.120
Monteith	WN	124	1.11	0.06	0.84	0.085	0.109
Monteith	Wn	119	0.07[a]	0.08	0.82	0.095	0.113
Monteith	wN	118	1.08[a]	0.07	0.76	0.092	0.127
Monteith	wn	124	1.11	0.08	0.76	0.112	0.143

[a]Slopes or intercepts not significantly different from 1.0 or 0.0, respectively ($\alpha = 0.05$).
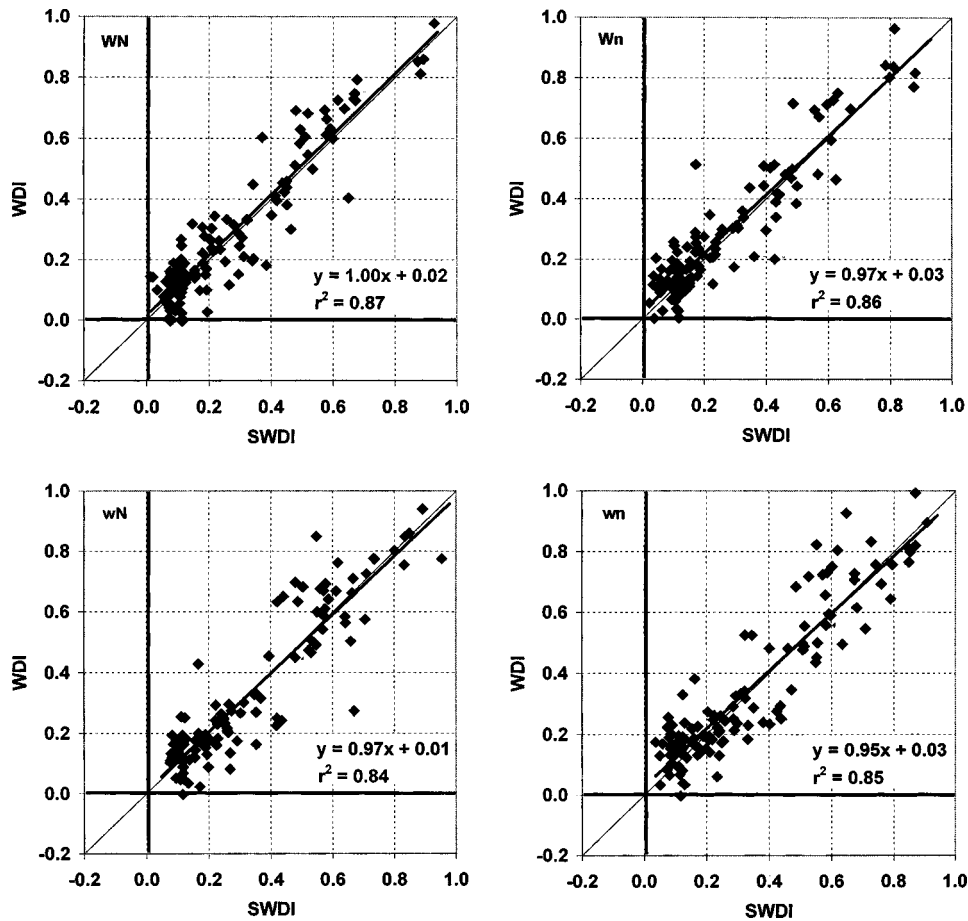
Fig. 1. Scattergram of water defecit index (no stability correction) versus soil water defecit index (Food and Agricultural Organization Paper 56 K_s) for each treatment

depths applied, and rainfall for Plot 12 (optimal water, optimal nitrogen WN) and Plot 16 (acute water stress, optimal nitrogen wN). The WDI and SWDI early in the season were both greater than typical mid-season values when canopy cover was full, even when water stress was not present. Before mid-season, more soil was exposed, but the drop hoses of the linear move system only wet 10–20% of the surface throughout the season. A greater portion of dry soil was viewed by the IRT on AgIIS, and dry soil has a greater temperature than wet soil, corresponding to higher WDI values. For the SWDI, the soil evaporation coefficient K_e in Eq. (8) is affected by the portion of soil wetted by irrigation. The $K_{c\text{-max}}$ term, however, is affected only by atmospheric demand and describes a completely wet soil and canopy surface composite (Allen et al. 1998). Therefore, $(K_{cb}K_s + K_e)$ will always be less than $K_{c\text{-max}}$, causing a corresponding increase in the SWDI. A reverse trend begins at the end of the season when leaf drop begins to expose the soil; however, leaf drop and age also reduces crop transpiration and increases canopy temperature (Jackson 1982), therefore increasing the WDI. This is accounted for by the K_{cb} term in Eq. (8), causing a corresponding increase in the SWDI. Thus, WDI or SWDI values greater than zero do not necessarily indicate that the crop is experiencing water stress.

Water was withheld from the acute water stress (w) treatment plots on DOY 193, 208, 223, 228, and 242. These plots received supplemental irrigations on DOY 214, 216, and 250 to reduce differences in total seasonal applications. Fig. 2 shows periods of water stress where both the WDI and the SWDI increased above the minimal possible values described above. On DOY 202, for

example, both Plots 12 and 16 exhibited elevated WDI and SWDI values that reflect a 5 day interval since the last irrigation (DOY 197). The water treatments also appear to have influenced f_c. In Plot 12, f_c reaches a seasonal maximum earlier (around DOY 210) than in Plot 16 (around DOY 230). The period from DOY 193 to 202 also suggests the effect of water stress on f_c as detected by the NDVI. After DOY 193, f_c begins to decline more sharply in Plot 16 than in Plot 12, likely the result of severe leaf wilt exposing more soil background (Jackson et al. 1986) in Plot 16. A 35 mm irrigation was applied to all plots on DOY 203, and f_c then returns to a general upward trend.

Fig. 3 shows AgIIS images of the WDI on DOY 202, 208, and 209. On DOY 193, only the optimal water (W) plots were irrigated; however, the effects were not immediately observed because 25 mm of rain fell on DOY 195. By DOY 202, each water treatment is fairly distinguishable (5 days since irrigation for all plots), but distinctions become more obvious on DOY 209, where the optimal water (W) plots had been irrigated on the previous day. On DOY 208, 4 days had elapsed for all plots since the last irrigation. Distinctions between water treatments on this day were less obvious; nonetheless, most of the areas in the acute water stress (w) plots generally exhibited the higher WDI values. The effects of withholding the irrigation on DOY 193 could be detected by the WDI after 15 days, despite 25 mm on DOY 195. Although there is some disagreement between the WDI and the SWDI, each WDI plot average had the same relative rank as the SWDI. Jaynes and Hunsaker (1989) reported that spatial patterns of volumetric soil moisture point measurements tended to retain
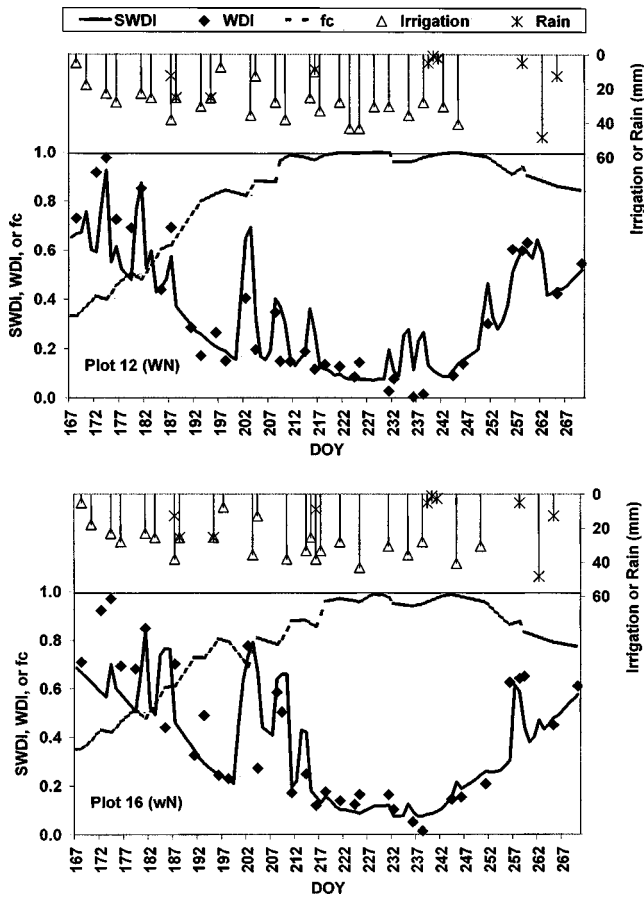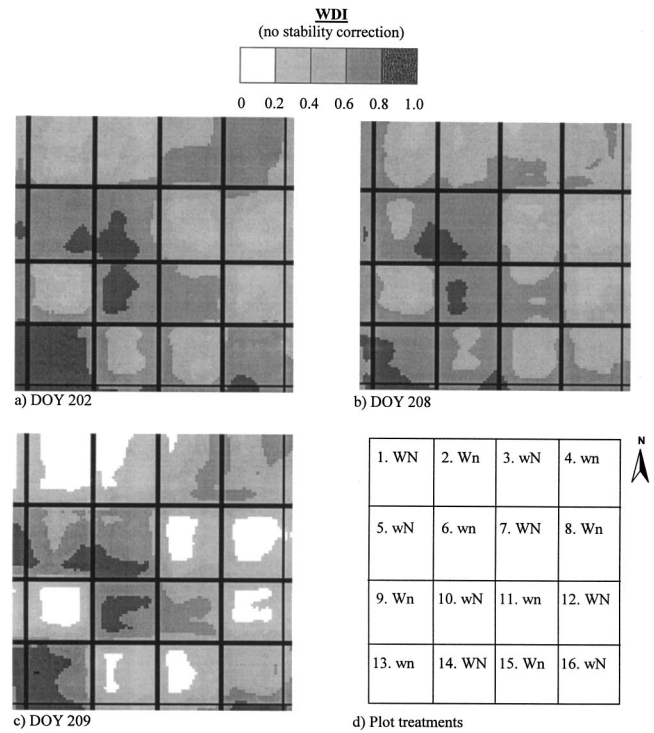
Fig. 2. Time series of soil water defect index (Food and Agricultural Organization Paper 56 K_s), water defect index (no stability correction), fraction of vegetation cover f_c, irrigation applications, and rainfall events

Fig. 3. Agricultural irrigation imaging system field images of water defect index (no stability correction): (a) DOY 202 (5 days since irrigation, all plots); (b) DOY 208 (4 days since irrigation, all plots); (c) DOY 209 (1 and 5 days since irrigation for W and w plots, respectively); and (d) plot treatments

their relative ranks across level basins before and after surface irrigations. We speculate that images such as those provided by AgIIS, when applied on a larger scale, may provide a visual aid for prioritizing irrigation schedules. Furthermore, WDI images could alert an irrigation manager to water stress that may not be apparent from visual assessments made from the ground along the perimeter of a field.

The fDEP is a key parameter for irrigation management (Colaizzi et al. 2003). Conceivably, fDEP could be estimated by substituting the WDI for the SWDI in Eq. (8) and solving for K_s. The FAO 56 K_s model could then be inverted to solve for fDEP. Colaizzi et al. (2003) reported reasonable estimates of fDEP using this approach with the CWSI in a similar study with cotton under low frequency irrigation at the same location. When this approach was applied in the present study, however, poor correlation ($r^2 < 0.40$) resulted between fDEP estimated from the WDI and that estimated from in situ soil moisture measurements.

Fig. 4 shows the relationship between K_s and fDEP. The K_s data points were calculated by substituting the WDI for the SWDI in Eq. (8) and solving for K_s. The K_s values are grouped into four atmospheric demand ET_p ranges. The Jensen and FAO 56 K_s models are shown, where three threshold (p) values are given for the FAO 56 model. When atmospheric demand was high (i.e., $ET_p = 11-13$ mm day^{-1}), the K_s point data tended to follow the FAO 56 model for the lower p thresholds. This may explain the slightly better correlation between WDI and SWSI using the FAO

56 K_s model compared to the Jensen model, which does not account for atmospheric demand but does account for slight water stress for lower fDEP. For $ET_p < 11$ mm day^{-1}, the relationship between K_s and fDEP is less unique. The K_s points further illustrate that soil moisture was maintained at relatively high levels (i.e., fDEP was less than about 0.6 for most measurements) because irrigations were small and frequent using the linear move system, and that K_s was relatively insensitive when fDEP is less than 0.6. Therefore, small errors in K_s using the WDI result in large errors in fDEP. In addition, estimates of K_s are subject to error in the WDI, K_{cb}, K_e, and $K_{c\text{-max}}$ terms according to Eq. (8),
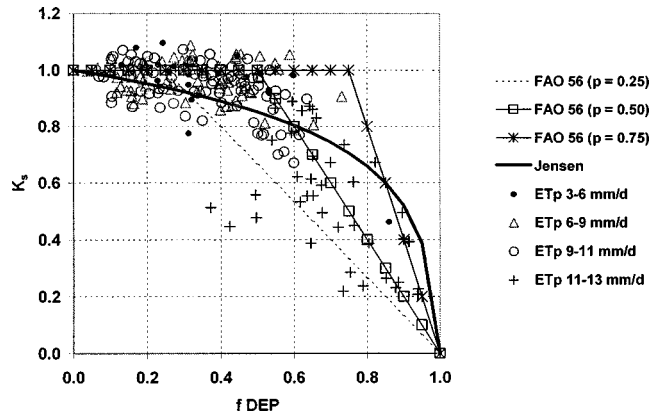
Fig. 4. Water stress coefficient K_s versus fraction of soil moisture depletion with points at several ranges of potential evapotranspiration (ET_p).

whereas estimates of K_s using the CWSI (valid only for no soil background) do not involve the K_{cb}, K_e, and $K_{c\text{-max}}$ terms. Consequently, estimates of fDEP using the WDI under high frequency irrigation correlated poorly to in situ soil moisture measurements. Furthermore, the use of canopy temperature to estimate fDEP may be limited to low frequency irrigation where a greater range of soil moisture is possible.

Finally, although the FAO 56 K_s model resulted in slightly better correlation between the WDI and the SWDI than the Jensen K_s model in the present study, Colaizzi et al. (2003) found that the FAO 56 K_s model resulted in much poorer correlation than the Jensen K_s model. Their study used low frequency surface irrigation, a much larger range of fDEP resulted, and perhaps different root growth patterns (Doorenbos and Kassam 1979). The FAO 56 K_s model in their study appeared to underestimate slight water stress when soil moisture was relatively plentiful, but overestimate water stress when soil moisture was limited or atmospheric demand was high. Thus, cotton under low frequency surface irrigation may have a different water stress response to fDEP and atmospheric demand than cotton under high frequency irrigation.

Conclusions

The AgIIS was suitable for providing red and NIR reflectance and thermal infrared measurements required for the WDI. The WDI was sensitive to differences in water treatments from partial to full canopy cover during the 1999 season in Maricopa, Ariz.

The SWDI was derived using the K_{cb}, K_s, K_e, and $K_{c\text{-max}}$ coefficients in the FAO 56 dual crop coefficient procedure, where K_s is a function of fDEP and ET_c (or solely fDEP in the Jensen K_s function). The FAO 56 K_s model resulted in slightly better correlation between the WDI and the SWDI than the Jensen K_s model. Atmospheric stability correction for the WDI did not improve correlation. The comparisons linked the WDI to soil moisture through the K_s term.

The WDI was used to estimate fDEP through the K_s term; however, these estimates were poorly correlated to those from in situ soil moisture measurements. With high frequency irrigation, fDEP is maintained at a relatively lower range where K_s is less sensitive; therefore, small errors in K_s result in large errors in estimating fDEP, particularly when $K_s = 1$ using the FAO 56 model. The use of a canopy temperature based index to estimate fDEP may be more feasible under low frequency irrigation where there is a larger range of soil moisture. The Jensen K_s model may also be more appropriate for low frequency irrigation because it accounts for slight water stress when soil moisture is relatively plentiful (Colaizzi et al. 2003); however, future studies should investigate possible refinements to the K_s–fDEP relation for different irrigation regimes.

Disagreement between the WDI and the SWDI may have been related to the instantaneous nature of the former compared to the average daily nature of the latter. In addition, the relationship between canopy temperature and soil moisture is not always unique because the former may be influenced by root volume, intermittent clouds, and the cooling effects of precipitation.

The detection of water stress in terms of an index may aid in timing irrigations but does not indicate optimal water depths to apply. The high spatial-resolution field images of the WDI provided by AgIIS could nonetheless aid in site-specific crop management by showing areas of water stress that otherwise may not be visible from ground observations along a field perimeter. This information would be crucial for irrigation management and could potentially improve water use efficiency. Research using AgIIS for other crops is presently underway at the study location.

Appendix. Calculation of Water Deficit Index Temperature Components

The four $(T_s - T_a)_n$ terms in Eqs. (2) and (3) are based on the same energy balance principles used in defining the upper and lower limits of the CWSI (Jackson et al. 1981). The WDI also considers wet and dry bare soil. The four terms are (Moran et al. 1994)

$$(T_s - T_a)_{wv} = \frac{r_{a1}(R_{n1} - G_1)}{\rho_a C_p} \frac{\gamma_1(1 + r_{cp}/r_{a1})}{\Delta_1 + \gamma_1(1 + r_{cp}/r_{a1})}$$
$$- \frac{VPD}{\Delta_1 + \gamma_1(1 + r_{cp}/r_{a1})} \qquad (9)$$

$$(T_s - T_a)_{dv} = \frac{r_{a2}(R_{n2} - G_2)}{\rho_a C_p} \frac{\gamma_2(1 + r_{cx}/r_{a2})}{\Delta_2 + \gamma_2(1 + r_{cx}/r_{a2})}$$
$$- \frac{VPD}{\Delta_2 + \gamma_2(1 + r_{cx}/r_{a2})} \qquad (10)$$

$$(T_s - T_a)_{ws} = \frac{r_{a3}(R_{n3} - G_3)}{\rho_a C_p} \frac{\gamma_3}{\Delta_3 + \gamma_3} - \frac{VPD}{\Delta_3 + \gamma_3} \qquad (11)$$

$$(T_s - T_a)_{ds} = \frac{r_{a4}(R_{n4} - G_4)}{\rho_a C_p} \qquad (12)$$

where wv = wet vegetation (well-watered canopy); ws = wet bare soil; dv = dry vegetation (completely water stressed canopy); ds = dry bare soil, r_a = aerodynamic resistance (s m^{-1}); R_n = net incoming radiant flux density (W m^{-2}); G = soil heat flux density (W m^{-2}); ρ_a = density of dry air (1.19 kg m^{-3}); C_p = specific heat of dry air (1013 J kg^{-1} °C^{-1}); γ = psychrometric parameter (kPa °C^{-1}); Δ = slope of the saturated vapor pressure–temperature relation (kPa °C^{-1}); r_{cp} is the canopy resistance at potential transpiration (unlimited water); and r_{cx} = upper limit of canopy resistance (completely stressed). The r_a term was computed using the Campbell model (with or without stability correction) or the Monteith model (Colaizzi et al. 2003). The r_{cp} and r_{cx} terms for cotton were assumed constant at 10 and 250 s m^{-1}, respectively (Ehrler 1973; Keener and Gardner 1987).

Jensen et al. (1990) give procedures to calculate e_a^*, γ, and Δ; these require T_a as inputs. Jackson et al. (1981) recommend replacing T_a by the average of T_a and T_c (canopy temperature) in calculating γ and Δ for the CWSI. This was applied to the WDI for each surface by replacing T_a with the average of T_a and T_s. The γ and Δ terms therefore become slightly different for each corner because T_s are different, hence the subscripts for the γ and Δ terms. Since T_s now appears on both sides of Eqs. (9), (10), and (11), a solution by iteration is necessary.

For each surface (VI/T corners), R_n was assumed to be a fraction of total incoming short-wave solar radiation R_s, and G a fraction of R_n (Moran et al. 1994)

$$\begin{array}{lll} R_{n1}=0.7R_s & G_1=0.1R_{n1} & C_1 \\ R_{n2}=0.7R_s & G_2=0.1R_{n2} & C_2 \\ R_{n3}=0.7R_s & G_3=0.3R_{n3} & C_3 \\ R_{n4}=0.5R_s & G_4=0.3R_{n4} & C_4 \end{array} \qquad (13)$$

References

Allen, R. G., Pereira, L. S., Raes, D., and Smith, M. (1998). "Crop evapotranspiration." *Irrigation and Drainage Paper No. 56*, Food and Agricricultural Organization of the United Nations, Rome.

Arizona Meterological Network (AZMET). (1999). *The Arizona meteorological network*, ⟨http://ag.arizona.edu/AZMET⟩ (Oct. 15, 1999).

Clarke, T. R. (1997). "An empirical approach for detecting crop water stress using multispectral airborne sensors." *Hort. Tech.,* 7(1), 9–16.

Colaizzi, P. D. (2001). "Ground-based remote sensing for irrigation management in precision agriculture." PhD dissertation, The Univ. of Arizona, Tucson, Ariz.

Colaizzi, P. D., Barnes, E. M., Clarke, T. R., Choi, C. Y., and Waller, P. M. (2003). "Estimating soil moisture under low frequency surface irrigation using the crop water stress index." *J. Irrig. Drain. Eng.,* 129(1), 27–35.

Doorenbos, J., and Kassam, A. H. (1979). "Yield response to water." *Irrigation and Drainage Paper No. 33*, Food and Agricultural Organization of the United Nations, Rome.

Ehrler, W. (1973). "Cotton leaf temperatures as related to soil water depletion and meteorological factors." *Agron. J.,* 65, 404–409.

Ellsworth, P. C., and V. Barkley. (2001). "Cost-effective *Lygus* management in Arizona cotton." *Proc., Beltwide Cotton Conf.*, Vol. 2, P. Dugger and D. Richter, eds., National Cotton Council, Memphis, Tenn., 1021–1025.

Huete, A. R. (1988). "A soil-adjusted vegetation index (SAVI)." *Remote Sens. Environ.,* 25, 295–309.

Idso, S. B., Jackson, R. D., Pinter, Jr., P. J., Reginato, R. J., and Hatfield, J. L. (1981). "Normalizing the stress-degree parameter for environmental variability." *Agric. Meterol.,* 24, 45–55.

Jackson, R. D. (1982). "Canopy temperature and crop water stress." *Advances in irrigation*, D. Hillel, ed., Vol. 1, Academic, New York, 43–85.

Jackson, R. D. (1984). "Remote sensing of vegetation characteristics for farm management." *Proc. SPIE,* 475, 81–96.

Jackson, R. D., Idso, S. B., Reginato, R. J., and Pinter, Jr., P. J. (1981).

"Canopy temperatures as a crop water stress indicator." *Water Resour. Res.,* 17, 1133–1138.

Jackson, R. D., Pinter, Jr., P. J., Reginato, R. J., and Idso, S. B. (1986). "Detection and evaluation of plant stresses for crop management decisions." *IEEE Trans. Geosci. Remote Sens.,* GE-24(1), 99–106.

Jaynes, D. B., and Hunsaker, D. J. (1989). "Spatial and temporal variability of water content and infiltration on a flood irrigated field." *Trans. ASAE,* 32(4), 1229–1238.

Jensen, M. E., Burman, R. D., and Allen, R. G. (1990). "Evapotranspiration and irrigation water requirements." *ASCE Manuals and Rep. on Engineering Practice No. 70*, ASCE, New York.

Jensen, M. E., Robb, D. C. N., and Franzoy, C. E. (1970). "Scheduling irrigations using climate-crop-soil data." *J. Irrig. Drain. Eng.,* 96(1), 25–38.

Keener, M. E., and Gardner, B. (1987). "CWSI and stomatal resistance of cotton and soybeans." *Proc., Irrigation and Drainage Division*, Portland, Ore., ASCE, New York, 560–567.

Kimes, D. S., Idso, S. B., Pinter, Jr., P. J., Reginato, R. J., and Jackson, R. D. (1980). "View angle effects in the radiometric measurement of plant canopy temperatures." *Remote Sens. Environ.,* 10, 273–284.

Kjelgaard, J. F., Stockle, C. O., and Evans, R. G. (1996). "Accuracy of canopy temperature energy balance for determining daily evapotranspiration." *Irrig. Sci.,* 16, 149–157.

Moran, M. S. (1994). "Irrigation management in Arizona using satellites and airplanes." *Irrig. Sci.,* 15, 35–44.

Moran, M. S., Clarke, T. R., Inoue, Y., and Vidal, A. (1994). "Estimating crop water deficit using the relation between surface-air temperature and spectral vegetation index." *Remote Sens. Environ.,* 49, 246–263.

Moran, M. S., Inoue, Y., and Barnes, E. M. (1997). "Opportunities and limitations for image-based remote sensing in precision crop management." *Remote Sens. Environ.,* 61, 319–346.

Phene, C. J., Howell, T. A., and Sikorski, M. D. (1985). "A traveling trickle irrigation system." *Advances in irrigation*, D. Hillel, ed., Vol. 3, Academic, Orlando, Fla., 1–49.

Post, D. F., Mack, C., Camp, P. D., and Suliman, A. S. (1988). "Mapping and characterization of the soils on the University of Arizona Maricopa Agricultural Center." *Proc., Hydrology and Water Resources in Arizona and the Southwest*, Vol. 18, Arizona–Nevada Academy of Science, Tucson, Ariz., 49–60.

Rouse, J. W., Haas, R. H., Schell, J. A., Deering, D. W., and Harlan, J. C. (1974). "Monitoring the vernal advancement and retrogradiation (greenwave effect) of natural vegetation." *Type III Final Rep., National Aeronautics and Space Administration (NASA)*, Goddard Space Flight Center, Greenbelt, Md.

Sadler, E. J., Evans, R. G., Buchleiter, G. W., King, B. A., and Camp, C. R. (2000). "Design considerations for site specific irrigation." *Proc., 4th Nat. Irrigation Symp.*, Phoenix, ASAE, St. Joseph, Mich., 304–315.